International Journal of Signal Processing, Image Processing and Pattern Recognition
Vol.8, No.8 (2015), pp.177-190
http://dx.doi.org/10.14257/ijsip.2015.8.8.20

Study of a Novel Micro-mechanical Gyroscope using for Rotation Carrier

Wang Hong-wei

Physics and mathematics institute, Beijing Information Science and Technology University. Beijing, and 100192, China
drhwh@biti.edu.cn; drwanghw@yeah.net

Abstract

In this paper, a novel silicon micro-machined gyroscope is introduced, which is driven by the rotating carrier's angular velocity. The principle of structure is analyzed .The mathematic module is also established and the dynamics parameters of the gyroscope is calculated, Design and analysis of signal processing circuit, design and processing of the gyroscope sensing head, at last, the gyroscope is tested, the test results and the theoretical analysis is consistent。

Keywords: *Micromechanics, Gyroscope, Angular velocity*

1. Introduction

With the increasing development of MEMS and inertial guidance technology, all kinds of micro-machined gyros have successfully developed and are gaining increasing popularity for shared use in military and civil applications [1–3]. According to the driving structure, a MEMS gyro can be divided into two types. One is a gyro with a driving structure, and another is gyros without driving structures. The vast majority of reported micro-machined rate gyroscopes utilize a vibratory proof mass suspended by flexible beams above a substrate. The primary working principle is to form a vibratory drive oscillator, coupled to an orthogonal sense accelerometer by the Coriolis force. Using anchor, the proof mass is suspended above the substrate, making the mass free to oscillate in two orthogonal directions-the drive and the sense directions [4–8].

This kind of gyro is difficult to design and manufacture and the cost is high. In order to avoid the difficulties brought about by the driving part, this paper puts forward a novel gyro that uses the rotation of the aircraft itself as a driving part. In this paper, the studied gyro, which has been fabricated on mono-crystalline silicon wafer by means of bulk micromachining manufacturability techniques, belongs to the gyro without driving structure class. Since there is no driving structure, the structure is simple and easy to process [9, 10]. This new gyro is used on rotating aircraft for flight attitude control. The gyro sensing element is called a silicon pendulum. Aircraft spin provides angular momentum for the silicon pendulum so that it can sense the transverse angular velocity when aircraft appears to turn. Using detection circuits, the angular vibration of the silicon pendulum is transformed into an alternating electric signal. The signal frequency is same as the spin frequency of aircraft, and the signal envelope is proportional to the transverse angular velocity.

2. Principle of Structure

Figure 1 shows the structure of the micro-machined silicon gyroscope derived by carrier's angular velocity. In Figure 1, 1 is silicon proof mass (sensing mass, mass),2 is silicon elasticity torsion girder, 3 is electrode. Four electrode and silicon proof mass form four capacitors. The coordinates *XYZ* is fixed on mass of sensor, $\dot{\alpha}$

ISSN: 2005-4254 IJSIP

is angular velocity about mass vibrating around the *OY* axes, $\dot{\varphi}$ is carrier's spin angular velocity, Ω is carrier's yaw or pitching angular velocity. The gyroscope is fixed on the carrier and rotates with the carrier at the speed, yawing or pitching with the speed Ω at the same time. The mass is affectted by coriolis force changing frequently (the frequent of the coriolis force equals to the frequent of carrier rotating), and then the mass oscillates along the *OY* axes. The oscillation causes capacitance variety of four capacitors.

(C_1 ,C_2 ,C_3 ,C_4) ,which are formed by the mass and four electrode. It is shown in Fig 2, variety of capacitance signal is converted into the variety of voltage signal and then the voltage signal is amplified, so we can obtain the voltage signal in proportion to the angular velocity Ω that we need detect.

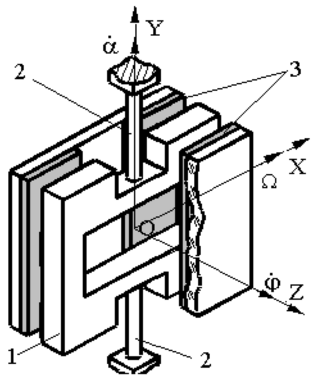

Figure 1. The Principle Structure of Sensor

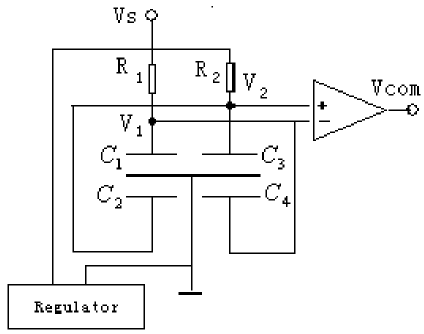

Figure 2. Principle of Signal Detecting Circuit

3. Dynamic Model

3.1 Vibration Equation of the Mass

The equation of vibration mass can be described by coordinate transform. In Figure 3, $O\xi\eta\zeta$ is the inertia coordinate (the fixed coordinate) $OX_1Y_1Z_1$ is the yaw or pitching coordinate; $OX_2Y_2Z_2$ is the spin coordinate of the carrier; $OXYZ$ is the coordinate connected on the mass. In the inertia coordinate $O\xi\eta\zeta$,

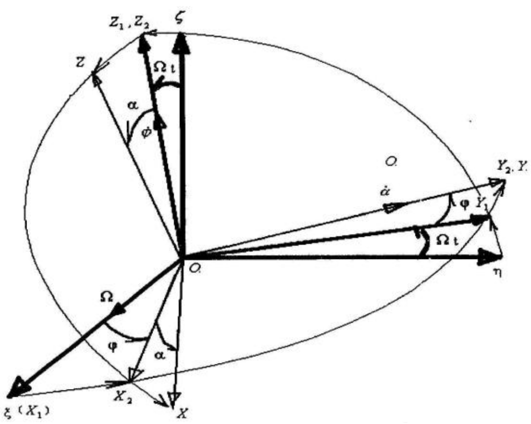

Figure 3. The Coordinate Transform

by the theory of angular momentum for rigid body rotating around fixed point , following formula can be obtained

$$\frac{d}{dt}\begin{bmatrix} G_\xi \\ G_\eta \\ G_\zeta \end{bmatrix} = \begin{bmatrix} M_\xi \\ M_\eta \\ M_\zeta \end{bmatrix} \tag{1}$$

in the formula, $\begin{bmatrix} G_\xi \\ G_\eta \\ G_\zeta \end{bmatrix} = J\begin{bmatrix} \omega_\xi \\ \omega_\eta \\ \omega_\zeta \end{bmatrix}$ is the angular momentum of the gyroscope mass in the coordinate $O\xi\eta\zeta$, $\begin{bmatrix} M_\xi \\ M_\eta \\ M_\zeta \end{bmatrix}$ is the moment which operates on the gyroscope mass in the coordinate $O\xi\eta\zeta$.

As the $OXYZ$ coordinate is set for inertia principal axis coordinate, rotating inertia matrix J is a constant value matrix.

(1) In inertial coordinate $O\xi\eta\zeta$, the mass rotates around $O\xi$ axis at the angular rate Ω and then turns angular Ωt to the coordinate $OX_1Y_1Z_1$, thus

$$\begin{bmatrix} G_\xi \\ G_\eta \\ G_\zeta \end{bmatrix} = A^{-1}\begin{bmatrix} G_{X_1} \\ G_{Y_1} \\ G_{Z_1} \end{bmatrix}, \begin{bmatrix} M_\xi \\ M_\eta \\ M_\zeta \end{bmatrix} = A^{-1}\begin{bmatrix} M_{X_1} \\ M_{Y_1} \\ M_{Z_1} \end{bmatrix}$$

in the formula, $A = \begin{bmatrix} 1 & 0 & 0 \\ 0 & \cos\Omega t & \sin\Omega t \\ 0 & -\sin\Omega t & \cos\Omega t \end{bmatrix}$ is transformation matrix, it is the function of time.

Putting the relation formula into the formula (1) and transforming, we can obtain that

$$\frac{d}{dt}\begin{bmatrix} G_{X_1} \\ G_{Y_1} \\ G_{Z_1} \end{bmatrix} + \begin{bmatrix} 0 & 0 & 0 \\ 0 & 0 & -\Omega \\ 0 & \Omega & 0 \end{bmatrix}\begin{bmatrix} G_{X_1} \\ G_{Y_1} \\ G_{Z_1} \end{bmatrix} = \begin{bmatrix} M_{X_1} \\ M_{Y_1} \\ M_{Z_1} \end{bmatrix} \tag{2}$$

(2) In the coordinate $OX_1Y_1Z_1$, the mass rotates around OZ_1 axis at the angular rate $\dot{\varphi}$ and then turns angular φ to the coordinate $OX_2Y_2Z_2$, thus

$$\begin{bmatrix} G_{X_1} \\ G_{Y_1} \\ G_{Z_1} \end{bmatrix} = B^{-1}\begin{bmatrix} G_{X_2} \\ G_{Y_2} \\ G_{Z_2} \end{bmatrix}, \begin{bmatrix} M_{X_1} \\ M_{Y_1} \\ M_{Z_1} \end{bmatrix} = B^{-1}\begin{bmatrix} M_{X_2} \\ M_{Y_2} \\ M_{Z_2} \end{bmatrix}$$

In the formula, $B = \begin{bmatrix} \cos\varphi & \sin\varphi & 0 \\ -\sin\varphi & \cos\varphi & 0 \\ 0 & 0 & 1 \end{bmatrix}$ is transformation matrix, it is the function of time.

Putting the formulation hereinbefore into the formulation (2), we can get that

$$\begin{bmatrix} 0 & -\dot{\varphi} & 0 \\ \dot{\varphi} & 0 & 0 \\ 0 & 0 & 0 \end{bmatrix}\begin{bmatrix} G_{X_2} \\ G_{Y_2} \\ G_{Z_2} \end{bmatrix} + \frac{d}{dt}\begin{bmatrix} G_{X_2} \\ G_{Y_2} \\ G_{Z_2} \end{bmatrix} + B\begin{bmatrix} 0 & 0 & 0 \\ 0 & 0 & -\Omega \\ 0 & \Omega & 0 \end{bmatrix} B^{-1}\begin{bmatrix} G_{X_2} \\ G_{Y_2} \\ G_{Z_2} \end{bmatrix} = \begin{bmatrix} M_{X_2} \\ M_{Y_2} \\ M_{Z_2} \end{bmatrix} \tag{3}$$

(3) In the coordinate $OX_2Y_2Z_2$, the mass rotates around OY_2 axis at the angular rate $\dot{\alpha}$ and then turns angular α to the coordinate $OXYZ$, thus

$$\begin{bmatrix} G_{X_2} \\ G_{Y_2} \\ G_{Z_2} \end{bmatrix} = C^{-1}\begin{bmatrix} G_X \\ G_Y \\ G_Z \end{bmatrix}, \begin{bmatrix} M_{X_2} \\ M_{Y_2} \\ M_{Z_2} \end{bmatrix} = C^{-1}\begin{bmatrix} M_X \\ M_Y \\ M_Z \end{bmatrix},$$

in the formula, $C = \begin{bmatrix} \cos\alpha & 0 & -\sin\alpha \\ 0 & 1 & 0 \\ \sin\alpha & 0 & \cos\alpha \end{bmatrix}$ is transformation matrix, it is the function of time.

Putting the formulation hereinbefore into the formulation (3), we can obtain that

$$\begin{bmatrix} 0 & \dot{\varphi} & 0 \\ \dot{\varphi} & 0 & 0 \\ 0 & 0 & 0 \end{bmatrix} C^{-1}\begin{bmatrix} G_X \\ G_Y \\ G_Z \end{bmatrix} + \frac{d}{dt}\left(C^{-1}\begin{bmatrix} G_X \\ G_Y \\ G_Z \end{bmatrix}\right) + B\begin{bmatrix} 0 & 0 & 0 \\ 0 & 0 & -\Omega \\ 0 & \Omega & 0 \end{bmatrix} B^{-1}C^{-1}\begin{bmatrix} G_X \\ G_Y \\ G_Z \end{bmatrix} = C^{-1}\begin{bmatrix} M_X \\ M_Y \\ M_Z \end{bmatrix}$$

After the formulation hereinbefore has been predigested, we can get that

$$\begin{bmatrix} 0 & -\Omega\cos\varphi\sin\alpha - \dot{\varphi}\cos\alpha & -\Omega\sin\varphi + \dot{\alpha} \\ \Omega\sin\alpha\cos\varphi + \dot{\varphi}\cos\alpha & 0 & \dot{\varphi}\sin\alpha - \Omega\cos\varphi\cos\alpha \\ \Omega\sin\varphi - \dot{\alpha} & \Omega\cos\varphi\cos\alpha - \dot{\varphi}\sin\alpha & 0 \end{bmatrix}\begin{bmatrix} G_X \\ G_Y \\ G_Z \end{bmatrix} + \frac{d}{dt}\begin{bmatrix} G_X \\ G_Y \\ G_Z \end{bmatrix} = \begin{bmatrix} M_X \\ M_Y \\ M_Z \end{bmatrix} \tag{4}$$

In the coordinate $OXYZ$, angular momentum of the gyroscope mass is

$$\begin{bmatrix} G_X \\ G_Y \\ G_Z \end{bmatrix} = J\begin{bmatrix} \psi_X \\ \psi_Y \\ \psi_Z \end{bmatrix} = \begin{bmatrix} J_X\psi_X \\ J_Y\psi_Y \\ J_Z\psi_Z \end{bmatrix}$$

in the formulation, J_X, J_Y, J_Z are the moments of inertia for the gyroscope mass in X ,Y, Z axises and ψ_X , ψ_Y , ψ_Z are projection component of the angular velocity vector in coordinate $OXYZ$.

$$\begin{bmatrix} \psi_X \\ \psi_Y \\ \psi_Z \end{bmatrix} = \begin{bmatrix} \Omega\cos\varphi\cos\alpha - \dot{\varphi}\sin\alpha \\ -\Omega\sin\varphi + \dot{\alpha} \\ -\Omega\cos\varphi\sin\alpha + \dot{\varphi}\cos\alpha \end{bmatrix}$$

Thus,

$$\begin{bmatrix} G_X \\ G_Y \\ G_Z \end{bmatrix} = J\begin{bmatrix} \psi_X \\ \psi_Y \\ \psi_Z \end{bmatrix} = \begin{bmatrix} J_X\psi_X \\ J_Y\psi_Y \\ J_Z\psi_Z \end{bmatrix} = \begin{bmatrix} J_X(\Omega\cos\varphi\cos\alpha - \dot{\varphi}\sin\alpha) \\ J_Y(-\Omega\sin\varphi + \dot{\alpha}) \\ J_Z(-\Omega\cos\varphi\sin\alpha + \dot{\varphi}\cos\alpha) \end{bmatrix}$$

Putting the formulation hereinbefore into the formulation (4), we can obtain three dynamic equations, the dynamic equation in OY axis is

$$\begin{aligned} &(J_X + J_Z)\Omega^2\cos^2\varphi\sin\alpha + (J_Z - J_X)\dot{\varphi}^2\sin\alpha\cos\alpha + J_X\Omega\dot{\varphi}\cos\varphi\cos 2\alpha - J_Z\Omega\dot{\varphi}\cos\varphi + \\ &J_Y\ddot{\alpha} - J_Y\Omega\dot{\varphi}\cos\varphi - J_Y\frac{d\Omega}{dt}\sin\varphi = M_Y \end{aligned} \tag{5}$$

The summation for moment of external force in OY axis is

$$M_Y = -K_T\alpha - D\dot{\alpha}$$

Considering $\Omega << \dot{\varphi}$, item Ω^2 can be neglected. As $\alpha = 0$,we can get $\sin\alpha \approx \alpha, \cos\alpha = \cos 2\alpha = 1$, Let

$$\frac{d\Omega}{dt} = 0 .$$

get following equation:

$$J_Y\ddot{\alpha} + D\dot{\alpha} + \left[\left(J_Z - J_X\right)\dot{\varphi}^2 + K_T\right]\alpha = (J_Z + J_Y - J_X)\Omega\dot{\varphi}\cos(\dot{\varphi}t) \qquad (6)$$

in the formulation hereinbefore, J_X, J_Y, J_Z are the moments of inertia for the gyroscope mass in X ,Y, Z axises, K_T is the coefficient of torsion rigidity, D is damping coefficient.

3.2 Solution of Angular Vibration Vibrating Equation

Reducing the formulation (6), we can obtain that

$$\ddot{\alpha} + 2\xi\omega_0\dot{\alpha} + \omega_0^2\alpha = f_0\cos(\dot{\varphi}t) \qquad (8)$$

In the formulation,

$$\omega_0^2 = \frac{1}{J_Y}\left[\left(J_Z - J_X\right)\dot{\varphi}^2 + K_T\right] \qquad (9)$$

$$\xi = \frac{D}{2\omega_0 J_Y} = \frac{D}{2\sqrt{\left[\left(J_Z - J_X\right)\dot{\varphi}^2 + K_T\right]J_Y}} \qquad (10)$$

$$f_0 = \frac{1}{J_Y}(J_Z + J_Y - J_X)\Omega\dot{\varphi}$$

Its solution is

$$\alpha = Ae^{-nt}\cos\left(\sqrt{\omega_0^2 - n^2}t + \delta\right) + B\cos\left(\dot{\varphi}t - \beta\right)$$

$$tg\beta = \frac{2n\dot{\varphi}}{\omega^2{}_0 - \dot{\varphi}^2}$$

A and δ are integration constant and can be defined by movement initial condition, B is amplitude for stable vibration, β is phase difference, phase vibration drops behind excitation force phase angular β, $n = \xi\omega_0$, it is damping factor.

The first part of the formulation hereinbefore is attenuated soon as the vibration time rising. The second part is determined by excitation force and its frequent equals to excitation force frequent (namely spin angular velocity of carrier), vibration amplitude is affected by not only excitation force but also excitation frequent and parameters of vibration system J_X, J_Y, J_Z, K_T, D. Stable solution for the equation is

$$a = B\cos\left(\dot{\varphi}t - \beta\right) = \frac{f_0}{\sqrt{(\omega^2{}_0 - \dot{\varphi}^2) + 4n^2\varphi^2}}\cos\left(\dot{\varphi}t - \beta\right)$$

Substituting parameters and reducing, we can get

$$\alpha = \frac{\left(J_Z + J_Y - J_X\right)\Omega\dot{\varphi}}{\sqrt{\left[\left(J_Z - J_X - J_Y\right)\dot{\varphi}^2 + K_T\right]^2 + \left(D\dot{\varphi}\right)^2}}\cos\left(\dot{\varphi}t - \beta\right)$$

Amplitude of angular vibration is

$$\alpha_m = \frac{(J_Z + J_Y - J_X)\dot{\varphi}}{\sqrt{\left[(J_Z - J_X - J_Y)\dot{\varphi}^2 + K_T\right]^2 + (D\dot{\varphi})^2}}\Omega \qquad (11)$$

4. Dynamic Parameter Analysis and Calculation

4.1 Torsion Rigidity Coefficient of Elastic Girder

The structure of elastic girder is shown in Figure 5, length, width and thickness of girder are L, W, and t. In order to be convenient for get the torsion rigidity coefficient of elastic girder, supposing:

(1) Turning angular is direct proportion to girder length;
(2) Warp of all brace girder 's cross-section are equal;
(3) Twist moments of girder's ends are equative, and their orientations are contrary.

According these assumptions, from elasticity mechanics we can get:

$$K = \frac{512Ga^3b}{\pi^4 L} \sum_{n=1,3,5....}^{\infty} \frac{1}{n^4}(1 - \frac{2a}{n\pi b}\tanh\frac{n\pi b}{2a}) \tag{12}$$

In the formulation, a and b are width and length of rectangle cross-section, G is shear modulus of material for girder.

From formulation (12) we get total rigidity of two girders.

$$K_T = 0.657 \times \frac{Gt^3w}{L} \sum_{n=1,3,5,......}^{\infty} \frac{1}{n^4}(1 - \frac{2t}{n\pi w}\tanh\frac{n\pi w}{2t}) \approx \frac{2}{3}\cdot\frac{Gt^3w}{L} \tag{13}$$

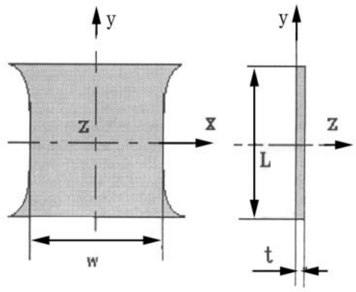

Figure 5. Structure of Supporting Girder

Put w=0.8mm, L=0.8mm, t=0.025mm, G=5.1×10^{10}（N/m^2）into the formulation (13), get

$$K_T = 5.313 \times 10^{-4} \mathrm{N \cdot m}.$$

4.2 Angular Vibration Damping Coefficient of Vibration Devices

When a rectangle plane with length A and width B moves towards underside whose gap breadth is H, the press membrane damping coefficient is

$$f = \frac{F_{damp}}{dh/dt} = \frac{AB^3\mu}{h^3}\left[1 - \frac{192B}{A\pi^5}\sum_{n=1.3.5...}\frac{1}{n^5}\tanh\frac{n\pi A}{2B}\right] \tag{14}$$

In the formulation, μ is gas adhesion coefficient, infinite series convergence is swiftness, so only get the first item, namely

$$f \approx \frac{AB^3\mu}{h^3}\left[1 - \frac{192B}{A\pi^5}\tanh\frac{\pi A}{2B}\right] \approx \frac{96\times\mu}{h^3.\pi^4}B^3A\left[1 - \frac{2}{\pi}\cdot\frac{B}{A}\tanh\left(\frac{\pi}{2}\cdot\frac{A}{B}\right)\right] \tag{15}$$

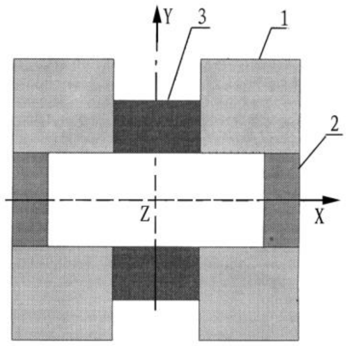

Figure 6. Damping Partition

As the structure of the vibrating mass is complex, calculating the damping coefficient is very difficult. For reducing the calculation difficulty, the gyroscope mass is divided into three areas with distinct colours, it is shown in Figure 6, then add damping of three district as the gyroscope vibration global damping approximately. Consult Figure 3, get angular vibration damping factor of three distinct are

$$D_1(d,\alpha)=\frac{4\times 96\mu}{\pi^4}\left[\frac{1}{(d+r_1\alpha)^3}+\frac{1}{(d-r_1\alpha)^3}\right]\left(\frac{b_3-b_2}{2}\right)^3\times\frac{a_3-a_1}{2}\left[1-\frac{2b_3-b_2}{\pi\alpha_3-\alpha_1}\tanh\left(\frac{\pi\alpha_3-a_1}{2b_3-b_2}\right)\right]r_1^2$$

$$D_2(d,\alpha)=\frac{2\times 96\mu}{\pi^4}\left[\frac{1}{(d+r_2\alpha)^3}+\frac{1}{(d-r_2\alpha)^3}\right]\left(\frac{a_3-a_2}{2}\right)^3\times b_2\left[1-\frac{1}{\pi}\frac{a_3-a_2}{b_2}\tanh\left(\pi\frac{b_2}{a_3-a_2}\right)\right]r_2^2$$

$$D_3(d,\alpha)=\frac{4\times 96\mu}{\pi^4}\left[\frac{1}{(d+r_3\alpha)^3}+\frac{1}{(d-r_3\alpha)^3}\right]\left(\frac{a_1}{2}\right)^3\times\frac{b_1-b_2}{2}\left[1-\frac{2}{\pi}\frac{a_1}{b_1-b_2}\tanh\left(\frac{\pi}{2}\frac{b_1-b_2}{a_1}\right)\right]r_3 \tag{16}$$

In the formulation,

$$r_1=\frac{a_3+a_1}{4},\quad r_2=\frac{a_3+a_2}{4},\quad r_3=\frac{a_1}{4}$$

Global damping factor of angular vibration is

$$D(d,\alpha)=D_1(d,\alpha)+D_2(d,\alpha)+D_3(d,\alpha)$$

Three relationship curves about damping coefficient and vibration angular are shown in Fig 7.

When d=0.017mm, d=0.020mm, d=0.023mm. From Fig 7, we get

D（2×10^{-5}，0）=1.231×10^{-5}($N\cdot m\cdot s$),

When d=0.020mm, a=0.

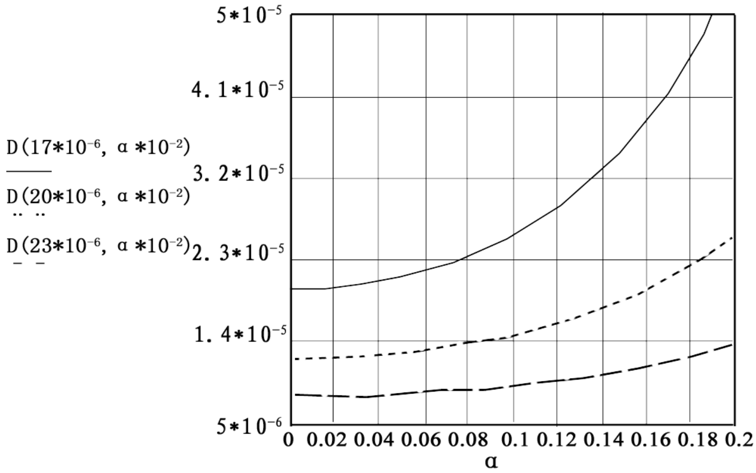

Figure 7. Relationship of Damping Coefficient and Swing Angle

5. Signal Detection

The signal detection circuit of micro-machined gyroscope is shown in Figure 3. When silicon pendulum spin with angular rate $\dot{\varphi}$, deflection angular α variation leads to four capacitors C1, C2, C3, C4 changing which are formed by silicon pendulum and electrode plane. The capacitance variety signal changes into voltage signal and the signal is amplified, getting the signal whose amplitude correspond to detected angular velocity.

Capacitance variety of micro-machined gyroscope is very small and be affected by distribution capacitance easily. So signal processing use alternating current bridge as transformation circuit of interface and capacitance sense device is used as operation arms of the bridge. The bridge supply is equivalency amplitude high frequent alternating voltage. When operation capacitors are changed, obtain the amplitude modulation wave signal modulated by operation capacitors variety at the output port of the bridge and signal is amplified and demodulated, then get low frequent output signal.

5.1 Signal Process Circuit

The signal process circuit is shown in Figure 8. Supply voltage stabilizer gives stable voltage to pulse generator in order to make pulse generator generate stable pulse signal. When inputted voltage of trigger reaches certain value, pulse generator begins turning from stillness stated to operation state, and as the input voltage fall to certain value,
generator turns from operation state to stillness state.

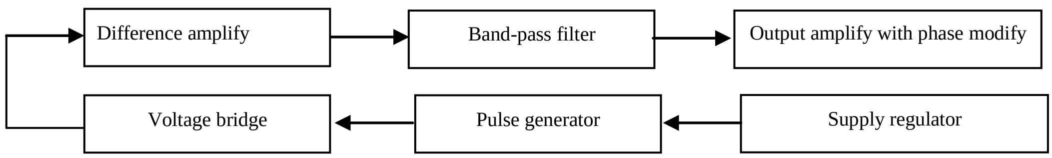

Figure 8. Sketch Map of Signal Process Circuit

The output signal through a feedback resister and a charging- discharging capacitor, then period rectangle wave U_{gen} can be obtained. At last, in the fig9, U_{gen} is voltage of signal picking up capacitor.

The capacitance-to-voltage conversion circuit is shown in Fig 10(a), namely capacitance-to-voltage conversion bridged, it consists of signal picking up capacitors C_{S_1} and C_{S_2} with variety clearance,

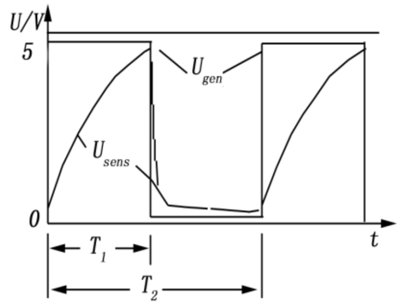

Figure 9. Impulse Builder and Voltage of Sense Capacitance

charging-discharging diodes D1, D2 and resisters R1, R2. The voltage U_{gen} generated by pulse generator is put on voltage input tip of bridge and charging-discharging diodes adjust the bridge performance. It is shown in Figure 10(b), the difference amplifier AD620 is an instrument amplifier consisted of three operation amplifiers, it's amplify multiple is determined by R_5 .

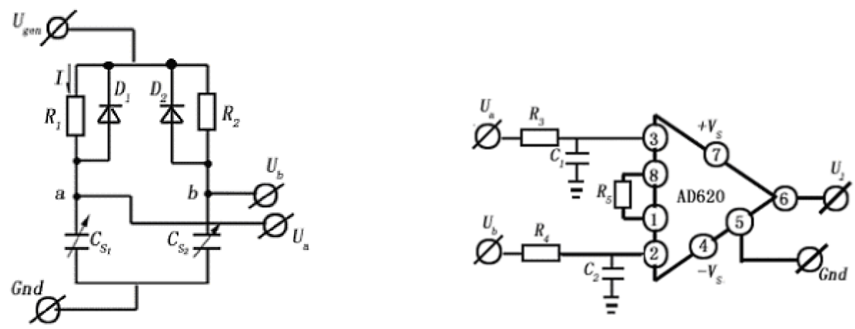

(a) Capacitance-to-voltage conversion circuit (b) Difference amplify circuit

Figure 10. Signal Process Schematic

5.2 Circuit Analysis

The pulse generator generates rectangle pulse voltage U_{gen}, whose high voltage is +5V and low voltage is 0V. The voltage is put on bridge, and then current through R_1、R_2 charging capacitors C_{S_1} and C_{S_2} The charging current also through reverse diodes, but this part of charging current is very small and can be neglected.

When t=0～T_1(U_{gen}=5V), capacitor's picking up voltage U_{gen} is decided by value of capacitor. When t=T_1~T (U_{gen}=0V), the voltage is decided by diode character and it approximates zero.

(1) As charging, namely

$$kT \leq t \leq kT + T_1 \quad k = 0, \pm 1, \pm 2 \cdots$$

the following expressions can be obtained.

$$U_a = U_m\left(1 - e^{-\frac{1}{R_1 C_{S_1}}}\right) \tag{17}$$

$$U_b = U_m\left(1 - e^{-\frac{1}{R_2 C_{S_2}}}\right) \tag{18}$$

In the formulation, U_m is amplitude of inspiriting signal U_{gen}.

(1) As discharging, namely

$kT + T \le t \le (k+1)T \qquad k = 0, \pm 1, \pm 2 \cdots$

Because forward resistance of diode is very small, charge of capacitor C_{S_1} is discharged instantly through diode, then U_a =0. During charging and discharging (t=0~T), the DC component of output voltage for a port is

$$\bar{U}_a = \frac{1}{T}\int_0^{T_1} U_\alpha dt = \frac{U_m}{T}\left[T_1 - R_1 C_{s1}\left(1 - e^{\frac{-T_1}{R_1 C_{S1}}}\right)\right] \tag{19}$$

Considering the structure of sensing device, let $C_{S_1} = C_0 - \Delta C$, $C_{S_2} = C_0 + \Delta C$, C_0 is inherence capacitor for electrode plane clearance with no Coriolis force, ΔC is capacitance variety with force. As $\Delta C << C_0$, $C_{S_1} = C_0 - \Delta C \approx C_0$ thus

$$\bar{U}_a \approx \frac{U_m}{T}\left[T_1 - R_1(C_0 - \Delta C)\left(1 - e^{\frac{-T_1}{R_1 C_0}}\right)\right] \tag{20}$$

Samely

$$\bar{U}_a \approx \frac{U_m}{T}\left[T_1 - R_2(C_0 + \Delta C)\left(1 - e^{\frac{-T_1}{R_2 C_0}}\right)\right] \tag{21}$$

Setting $R_1 = R_2$ thus

$$\bar{U}_{ab} \approx \bar{U}_\alpha - \bar{U}_b = \frac{2U_m R_1}{T}\left(1 - e^{\frac{-T_1}{R_1 C_0}}\right) \cdot \Delta C \tag{22}$$

The amplifier AD620 amplifies the output voltage of bridge

$$U_{out} = G\bar{U}_{ab} \tag{23}$$

In the formulation, G is the amplifier's amplification factor, G=49.4k$\Omega / R_5 + 1$.
The formulation (24) can be expressed

$$U_{out} = K\Delta C \tag{24}$$

In the formulation,

$$K = \frac{2U_m R_1}{T}\left(1 - e^{\frac{-T_1}{R_1 C_0}}\right) \cdot G \tag{25}$$

As R_1, R_2 and R_5 are selected values, G is constant value, T and T_1 are constant value decided by pulse generator and connected resisters and capacitors, inspiriting signal amplitude U_{gen} is decided by REF-02 and K is also constant value. The output signal has direct ratio with capacitance variety.

6. Gyroscope Sensor Structure and Processing Technology

6.1 "Sandwiches" Sensor

Gyro sensor is formed by the electrode on the top and the bottom and the vibration silicon modules in the middle, they form the "sandwiches" structure. As is shown in figure 11,the temperature expansion coefficient of silicon is 2.6×10^{-6}/℃.To ensure the stability of the "sandwich" structure, the temperature coefficient of expansion of the electrode has been closed with the temperature coefficient of expansion of the silicon. We choose the No. 75 ceramic Substrate.

Vibration silicon modules is shown in fig 12, the silicon quality is in the middle, outside are the frames, two flexible beams put the quality and the frames together. So that the quality can rotate around the axis consisted of two beams, the thickness of the frames are 30 um thicker than the thickness of the quality, so the two facets of the frame are 15 um higher than the two facets of the quality. The thickness of the beam is 48 um. There is prescribe hole in the center of mass of silicon, and 7 grooves outside, they are used to reduce the damping, the whole vibration modules is one structure through the micro-machined processing used the silicon as the material Figure 13 is the chart of the plates, blotted out regional in the map is copper electrode, electrode substrate are made by ceramics, the electrode on the top and the bottom and the vibration silicon modules in the middle formed the "sandwiches" sensor.

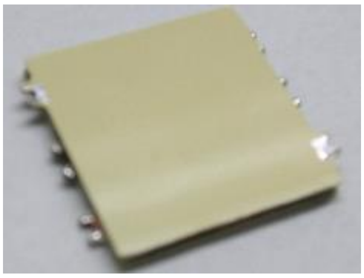

Figure 11. "Sandwiches"Sensor

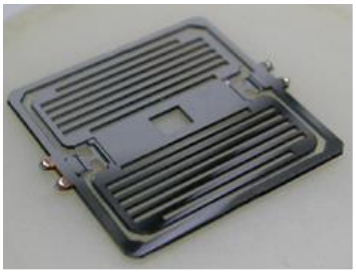

Figure 12, Vibration Silicon Modules

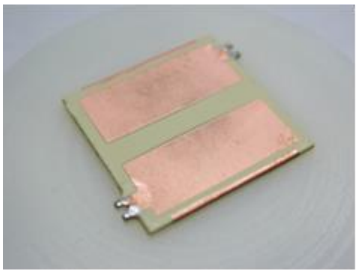

Figure 13. Chart of the Plates

6.2 Processing Technology of the Silicon Modules

Used for the 4-inch silicon, type N, double Polishing, (100) crystal face. In the experiment, we spent 30% of the concentration of KOH solution for corrosion, temperature is 104℃, corrosion rate is approximately 4.3. Process is shown in figure 14.

a. 2000 Å silicon dioxide layer double growth;
b. Double lithography, get rid of the oxide layer, get rid of the plastic;
c. 15um silicon surfaces of the deep corrosion each plane;
d. .5um silicon dioxide layer double growth;
e. Second double-lithography, 24um silicon surfaces of the deep corrosion each plane;
f. Third double-lithography, 80um silicon surfaces of the deep corrosion each plane;
g. Forth double-lithography, 64um silicon surfaces of the deep corrosion each plane, Link up.

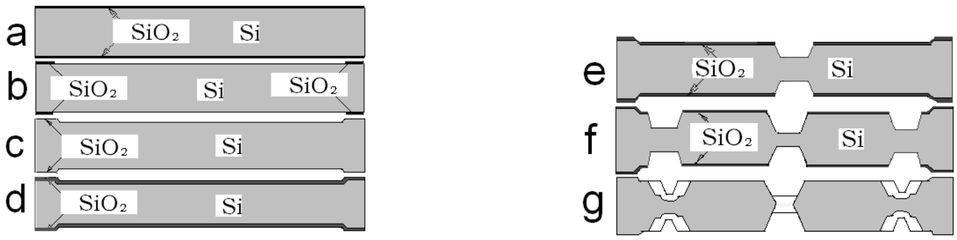

Figure 14. Processing Technology of the Silicon Modules

After seven steps above, we got the vibration silicon modules, But then the silicon beam vibration unit has not been processed out, next, the process is make the elastic beam of the silicon modules vibration. We put on a single silicon module for lithography, silicon corrosion, then, we got the vibration silicon modules, as is shown in Figure 12.

7. The Test of Gyroscope

The test was held on the test platform, shown in Figure 15. It was held on dynamic stand controlled by personal computer. The sensor rotation rate was set in the range 5 ~ 25 Hz by a rotation simulator. The tested sensors proved the total efficiency on all the conditions of the carried tests..
Dependence of the sensor output signal on the measured angular rate at different rotation frequencies of simulator is shown in Table 1 and Figure 16. Scale factor stability at changes of the measured angular rate is shown in Table 2.

Figure 15. Measuring Platform

Table 1. Dependence of the Sensor Output Signal on the Measured Angular Rate at Different Rotation Frequencies of Simulator

°/s Hz	50		100		150	
	CW.	**CCW**	**CW**	**CCW**	**CW**	**CCW**
12	**1.942**	**1.96**	**3.92**	**3.905**	**6**	**6**
17	**2.14**	**2.138**	**4.315**	**4.315**	**6.6**	**6.6**
22	**2.258**	**2.26**	**4.556**	**4.56**	**6.9**	**6.9**

Stability %	**±7.38**	**±7**	**±7.37**	**±7.6**	**±6.82**	**±6.82**

Table 2. Scale Factor Stability at Changes of the Measured Angular Rate

°/s / Hz	**50**		**100**		**150**		**Stability %**
	CW.	**CCW**	**CW**	**CCW**	**CW**	**CCW**	
12	**38.84**	**39.2**	**39.2**	**39.05**	**40**	**40**	**2.94**
17	**42.8**	**42.76**	**43.15**	**43.15**	**44**	**44**	**2.86**
22	**45.16**	**45.2**	**45.56**	**45.6**	**46**	**46**	**1.84**

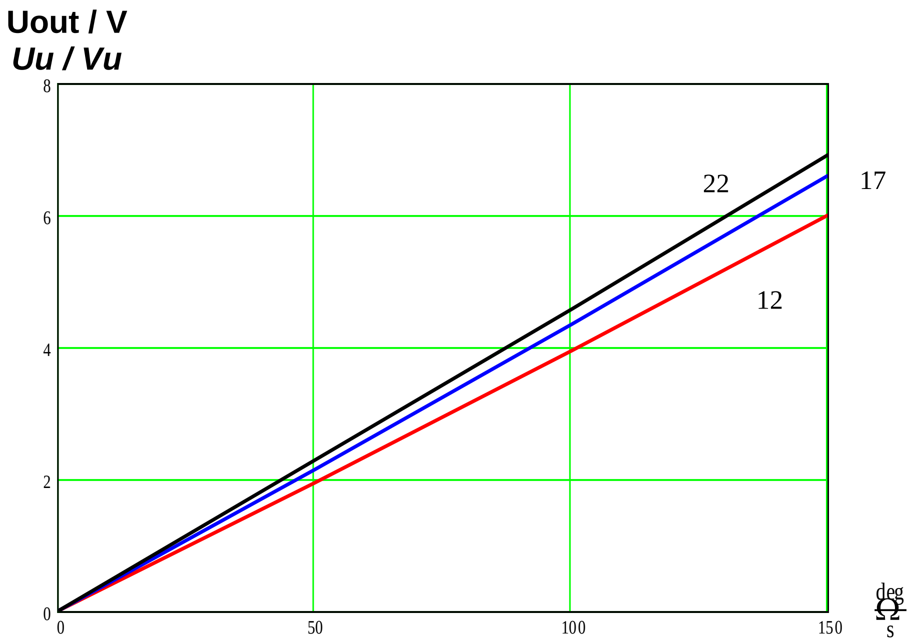

Figure 16. Dependence Gyroscope Output Signal from Input Rate (V)

8. Discussion and Conclusion

The influence of the rotate speed $\dot{\varphi}$ of the rotating substrate on proportional coefficient and output signals of the gyroscope is significant (up to 4.1%), because output signals of silicon micro-machined gyroscope is proportional to the rotate speed of the aircraft under low damp situation.to avoid the disadvantage which the rotate speed error caused by electron circuit makes output signals out of stability, the microprocessor in gyroscope modifies the rotating frequency achieved by measuring different angular rate, then the influence is decreased.

The instability of outputting damping coefficient D is mainly caused by varying of aerodynamic viscosity coefficient μ of gas in the case of the gyroscope according to temperature. For nitrogen, $\Delta\mu = 29.3\%$（100℃）, The variety of damping factor D because of varying temperature is ±17%. For low damp gyroscope, the main factor is the angular velocity of the rotating carrier itself $\dot{\varphi}$, not damping coefficient.

Using carrier's rotating angular velocity as driving force, and then forming micro-machined gyroscope without driving circuit and driving girder, this principle is correct.

Acknowledgements

This work was supported by

(1) The Opened Fund of the State Key Laboratory on Integrated Optoelectronics of China (Grant No. IOSKL2012KF13).

(2) Municipal key project of Natural Science Foundation of Beijing (B) (KZ201411232037).

(3) The development program of Beijing City Board of Education Science and Technology (KM201411232017) project.

References

[1] S.-H. Wang, "Current status and applications of MEMS sensors", Micronanoelectron. Technol., vol. 48, (**2011**), pp. 516–522.

[2] K. Liu and X. Tian, "Portable Air Defence Missile System Reliability Analysis and Design", In Proceedings of 2012 IEEE International Conference on Quality, Reliability, Risk, Maintenance, and Safety Engineering (ICQR2MSE), Brunow Palace, Poland, 25–29 June 2012, pp. 1171–1174.

[3] J. Hidalgo, P. Poulakis, J. Köhler, J. Del-Cerro and A. Barrientos, "Improving planetary rover attitude estimation via MEMS sensor characterization", Sensors, vol. 12, (**2012**), pp. 2219–2235.

[4] P. E. Conner, "MEMS Vibratory Gyroscopes: Structural Approaches to Improve Robustness", Springer: New York, NY, USA, (**1979**).

[5] M. Yoichi, T. Masaya and O. Kuniki, "A micromachined vidrating rate gyroscope with independent beams for the drive and detection modes", Sens. Actuators, vol. 80, (**2000**), pp. 170–178.

[6] W. Wang, X. Lv and F. Sun, "Design of a novel MEMS gyroscope array", Sensors, vol. 13, (**2013**), pp. 1651–1663.

[7] J. Raman, E. Cretu, P. Rombouts and L. Weyten, "A closed-loop digitally controlled MEMS gyroscope with unconstrained sigma-delta force-feedback", IEEE Sens. J., vol. 9, (**2009**), pp. 297–305.

[8] X. Z. Wu, L.-Q. Xie, J.-C. Xing, P.-T. Dong, H.-X. Wang and J.-B. Su, "A z-axis quartz tuning fork micromachined gyroscope based on shear stress detection", IEEE Sens. J., vol. 12, (**2012**), pp. 1246–1252.

[9] H. Wang, X. Mao, W. Zhang and F. Zhang, "The research and development of silicon micro machined gyroscope sensitive components of the rotation vector", The piezoelectric and acoustooptic, 2006 twenty-eighth volume second issue, p. 68.

[10] H. Wang, G. Teng, C. Qi and S. Y. Jiang, "Study on rotating silicon micro machined gyroscope, micro electronic technology", 7/8 Journal of 2007, pp. 284-288.

Author

Wang Hong-wei (1967-), he is in the study of gyroscope.

